J Mater Sci (2011) 46:3517–3522
DOI 10.1007/s10853-011-5260-y

Preparation of MnO_2/graphene composite as electrode material for supercapacitors

Yong Qian · Shunbao Lu · Fenglei Gao

Received: 8 July 2010 / Accepted: 6 January 2011 / Published online: 14 January 2011

Abstract MnO_2/graphene composite was synthesized by a facile and effective polymer-assisted chemical reduction method. The nanosized MnO_2 particles were homogeneously distributed on graphene nanosheets, which have been confirmed by scanning electron microscopy and transmission electron microscopy analysis. The capacitive properties of the MnO_2/graphene composite have been investigated by cyclic voltammetry(CV). MnO_2/graphene composite exhibited a high specific capacitance of 324 F g^{-1} in 1 M Na_2SO_4 electrolyte. In addition, the MnO_2/graphene composite electrode shows excellent long-term cycle stability (only 3.2% decrease of the specific capacitance is observed after 1,000 CV cycles).

Introduction

Supercapacitors, also called electrochemical capacitors (ECs) or ultracapacitors, have attracted considerable attention over the past decades because of their higher power density and longer cycle life than secondary batteries and their higher energy density compared to conventional electrical double-layer capacitors[1, 2]. To develop an advanced supercapacitor device, an active electrode material with high capacity performance is indispensable [3].

Graphene, with one-atom thick layer 2D structure, is emerging as a unique morphology carbon material with potential for electrochemical energy storage device applications due to its super characteristics of chemical stability, high electrical conductivity, and large surface area [4–6]. These encouraging characteristics provide such new materials a wide range of potential applications and have attracted great interests in developing graphene composites with other materials [7, 8].

Currently, one obvious challenge is to utilize these 2D carbon nanostructures as conductive carbon mats to anchor metal oxide materials to form new nanocomposite hybrid materials with potential application in optoelectronics and energy conversion devices. Paek et al. [9] fabricated the graphene/SnO_2 composite electrode materials and studied their application in lithium-ion batteries. Li et al. [10] reduced graphene oxide with $SnCl_2$ to gain graphene/SnO_2 composite which achieved a higher specific capacitance of 34.6 F/g in 1 M H_2SO_4 solution. Recently. Lu et al. [11] have reported that graphene/ZnO composite film was fabricated by ultrasonic spray pyrolysis and a higher specific capacitance about 11.3 F/g had been obtained by comparison to pure graphene or ZnO electrode. However, as promising hybrid electrode materials for ECs, the exploration on graphene-metal oxide composite materials is not nearly enough so far.

Among all the transition metal oxides, MnO_2 has been attracting research interest as it can be used in catalysis and electrochromic applications, and it is also electrochemical active in supercapacitors with a high-power nature [12–14]. Recently, Chen et al. [15] have reported that MnO_2/graphene

Y. Qian
Key Laboratory of Radioactive Geology and Exploration Technology Fundamental Science for National Defense, East China Institute of Technology, Fuzhou 344000, People's Republic of China

S. Lu
College of Life Science, Jiangxi Normal University, Nanchang 330027, People's Republic of China

F. Gao (✉)
Nanomaterials & Chemistry Key Laboratory, Wenzhou University, Wenzhou 325027, People's Republic of China
e-mail: jsxzgfl@sina.com

composite was prepared by direct redox reaction between MnO_4^- and Mn^{2+} on the graphene oxide as electrode material for supercapacitors. However, the capacitance of MnO_2/graphene composite had only 216 F g^{-1} and such method was a complicated, time/energy-consuming process.

In this article, MnO_2/graphene composite were synthesized by a facile and effective polymer-assisted chemical reduction method. The synthetic MnO_2/graphene composite have a uniform surface distribution and large coverage of MnO_2 nanoparticles onto graphene, MnO_2/graphene composite have a high specific capacitance of 324 F g^{-1}. The morphology and crystal structure of the composites were investigated by X-ray diffraction (XRD), scanning electron microscopy (SEM), and high-resolution transmission electron microscopy (TEM), respectively. The electrochemical properties of the MnO_2/graphene composite were investigated by cyclic voltammetry (CV) and the excellent capacitive properties were observed.

Experimental

In a typical synthesis process, natural graphite powders were oxidized to graphite oxide using a modified Hummers method [16]. Graphene nanosheets (GNS) were obtained by reduction of graphene oxide nanosheets (GONS) using hydrazine hydrate as a reducing agent at 100 °C for 2 h. A 30 mg sample of graphene and 30 mg poly(sodium 4-styrene sulfonate) (PSS, MW, 70,000) was mixed into 35 ml distilled water under stirring at 90 °C for 5 h, followed by addition of 40 mg $MnSO_4H_2O$, After another 1 h of stirring 100 μl of concentrated NH_3 and 480 μl of concentrated H_2O_2 were stepwise added into the mixture, and the resulting mixture was refluxed at 100 °C for 6 h. After being cooled to 50 °C, the suspension was filtered with a Millopore filter (pore diameter, 0.45 μm) and the product obtained was washed with distilled water and was dried at 100 °C under vacuum to give MnO_2/graphene composite.

The morphology and microstructure of the composites were characterized using SEM (FEI Sirion200) and TEM (Hitachi 9000). The crystallographic structures of the materials were determined by XRD (TTR-III) equipped with Cu Kα radiation. The capacitive properties of MnO_2/graphene electrode (the diameter (2 mm), the thickness (0.1 mm), the mass (1.58×10^{-4} g)) was investigated by CV in 1 M Na_2SO_4 (99,997%, Alfa Aesar) aqueous solutions on a electrochemical working station (CHI 660B).

Result and discussion

Figure 1a shows the SEM image of graphene nanosheets. As shown, the transparency of the graphene suggests a thin film over the entire substrate. The wrinkles observed were probably caused by the oxygen functionalization and the resultant defects during the preparation of graphene oxide (GO) [17]. Generally, graphene can attain large surface area owing to such unique two-dimensional structure, which allows the sheets to adjust themselves physically to adapt the different types of electrolytes [18, 19]. From tapping-mode, AFM image in Fig. 1c, it can be seen that the thickness of the GO is about 1.3 nm, which demonstrates that the graphene oxide sheets exist as one layer carbon sheet. We also performed the BET surface area measurement on pure graphene nanosheets by N_2 adsorption. The pure graphene nanosheets have a specific BET surface area of 93.7 m^2/g. Figure 1b is the SEM image of PSS-assisted synthesized MnO_2/graphene composite. The graphene nanosheets were covered by densely packed and homogeneous MnO_2. Figure 1d is the typical TEM image of graphene/MnO_2 composite. As shown in this figure, the sizes of the MnO_2 are in the range of 10–20 nm and have a good distribution as well as a high surface coverage onto graphene. PSS used here as the polymer to assist the synthesis of the composites serves as a bifunctional molecule both for solubilizing graphene into an aqueous solution and for tethering Mn^{2+} precursor onto graphene surfaces to facilitate the follow-up chemical deposition of MnO_2 to eventually on-spot grow MnO_2 nanoparticles onto graphene.

The phases of the prepared MnO_2/graphene composite were investigated by the XRD analysis, and the XRD pattern of the prepared MnO_2/graphene was shown in Fig. 2. The peaks at 2θ around 26° and 44.5° correspond to the (0 0 2) and (1 0 0) crystal plane of graphene, the peaks at 28.8°, 32.80°, 34.40°, 38.80°, 42.60°, 44.30°, and 65.50°, as shown in the XRD pattern of MnO_2/graphene film, correspond to the (3 1 0), (0 3 1), (1 3 1), (5 2 1), and (0 0 2) planes of MnO_2, respectively. All the reflection peaks of the products can be indexed as pure MnO_2 which is in good agreement with the literature values. No any other impurities were detected, which further proved the high pure MnO_2 deposits were successfully prepared [20, 21].

CV is considered to be a suitable tool to characterize the capacitive behavior of the electrode materials [22]. A large-current, rectangular-type CV and symmetry in anodic and cathodic directions are the indications of the ideal capacitive behavior of the electrode materials. Figure 3a shows the typical CVs of the as grown graphene (curve 1) and MnO_2/graphene composite(curve 2) electrodes at a scan rate of 50 mV s^{-1} in 1 M Na_2SO_4 aqueous solution under a potential range from 0 to 1 V. It can be seen that the MnO_2/graphene composite electrode has a near rectangular-shaped and symmetric CV, and its CV current density is much larger than that of the as grown graphene electrode. These suggest that the capacitive behavior

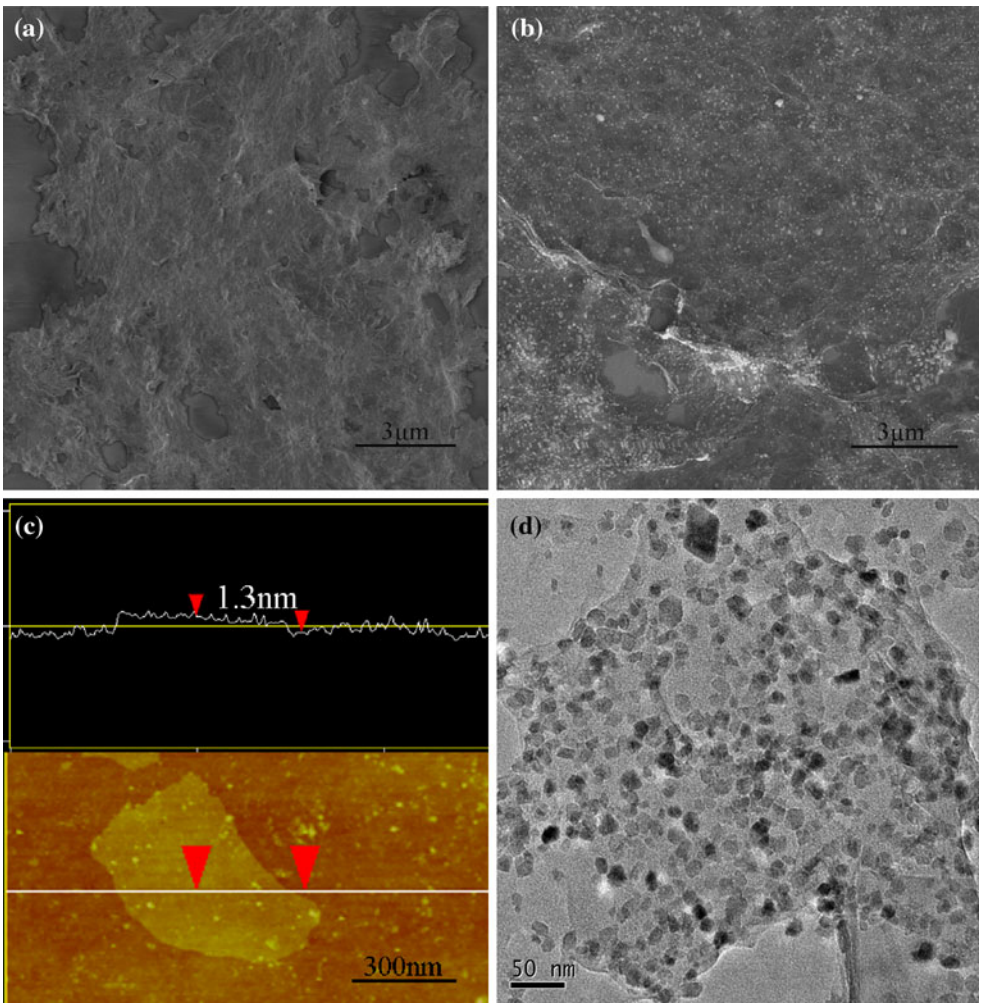

Fig. 1 SEM images of **a** as-synthesized graphene and **b** graphene/MnO_2 composite film. **c** Tapping-mode AFM image of graphene oxide and height profile plot showing the 1.3 nm thickness for individual graphene oxide sheets. **d** TEM image of MnO_2/graphene

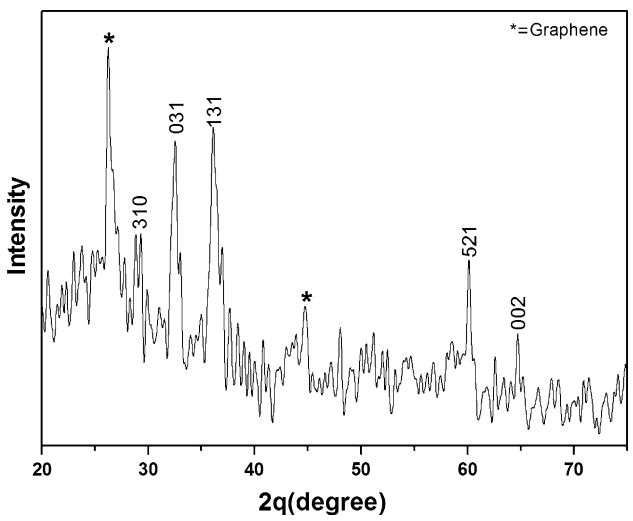

Fig. 2 XRD patterns of the MnO_2/graphene composite

shown in curve 2 is mainly because of the existence of MnO_2 layer and the MnO_2/graphene composite electrode has excellent capacitive performance.

It is well known that a rectangular-shaped CV over a wide range of scan rate is very important in supercapacitors for their practical capacitive application. The CVs of the MnO_2/graphene composite electrode at different scan rate are shown in Fig. 3b. As seen in Fig. 3b, the CV current density increases gradually with the increase of the scan rate of CV, but the curves do not have ideal rectangular shape. Why this material doesnot have rectangular CV curves? So far, we cannot know the exact reason about this result, and we just can figure out a possible one. In this article, PSS is used to assist the MnO_2 nanoparticle to deposit onto graphene. However, the polymer PSS's electrical conductivity is poor, which slows down the electron transfer of the anodic reaction, therefore the anodic peak is not evident and the CV curves are not ideally rectangular and symmetrical.

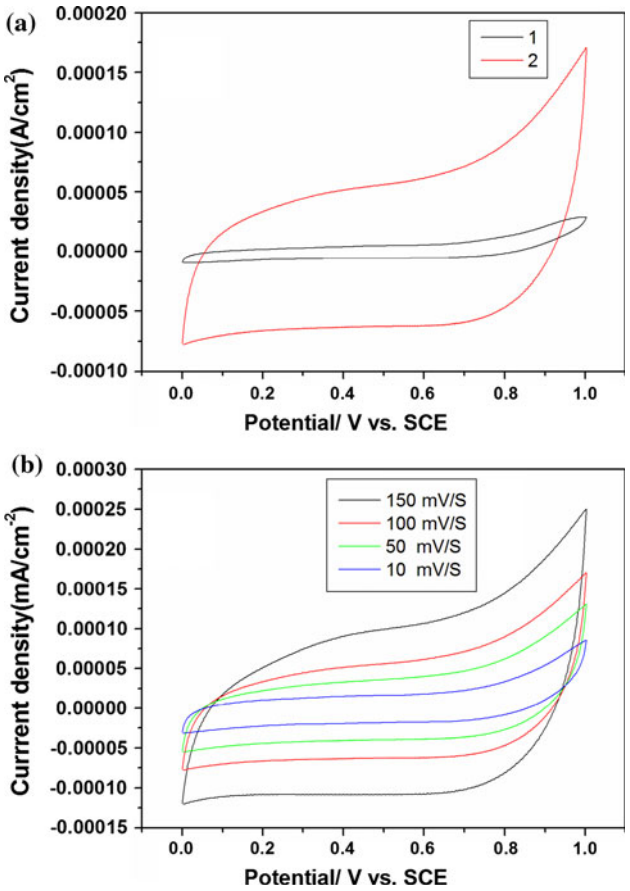

Fig. 3 **a** CV of the graphene (curve 1) and MnO_2/graphene composite (curve 2) electrodes at a scan rate of 100 mV s^{-1} in 1 M Na_2SO_4 aqueous solutions; **b** CV of the MnO_2/graphene composite electrode in 1 M Na_2SO_4 aqueous solutions at different scan rate. (1) 10 mV s^{-1}; (2) 50 mV s^{-1}; (3) 100 mV s^{-1}; (4) 150 mV s^{-1}

The dependence of the CV current density and the calculated value of the specific capacitance of the MnO_2/graphene composite electrode on scan rate of CV are shown in Fig. 4a and b. The specific capacitance (C_s) of the MnO_2/graphene composite electrode based on MnO_2 is calculated according to the following equation:

$$C_s = \frac{\int i dV}{vMV}$$

where i is the CV current density of the MnO_2/graphene composite electrode at 0.5 V in the CV anodic branch, V is the potential (V), v is the CV scan rate, and M is the mass of MnO_2/graphene composite. In this article, the contribution of graphene to the specific capacitance of the composite electrode is very low (curve 1 in Fig. 3a) and can be ignored in the calculation. From Fig. 4b, it is noteworthy that a specific capacitance as high as 324 F g^{-1} is obtained at a scan rate of 10 mV s^{-1} and a specific

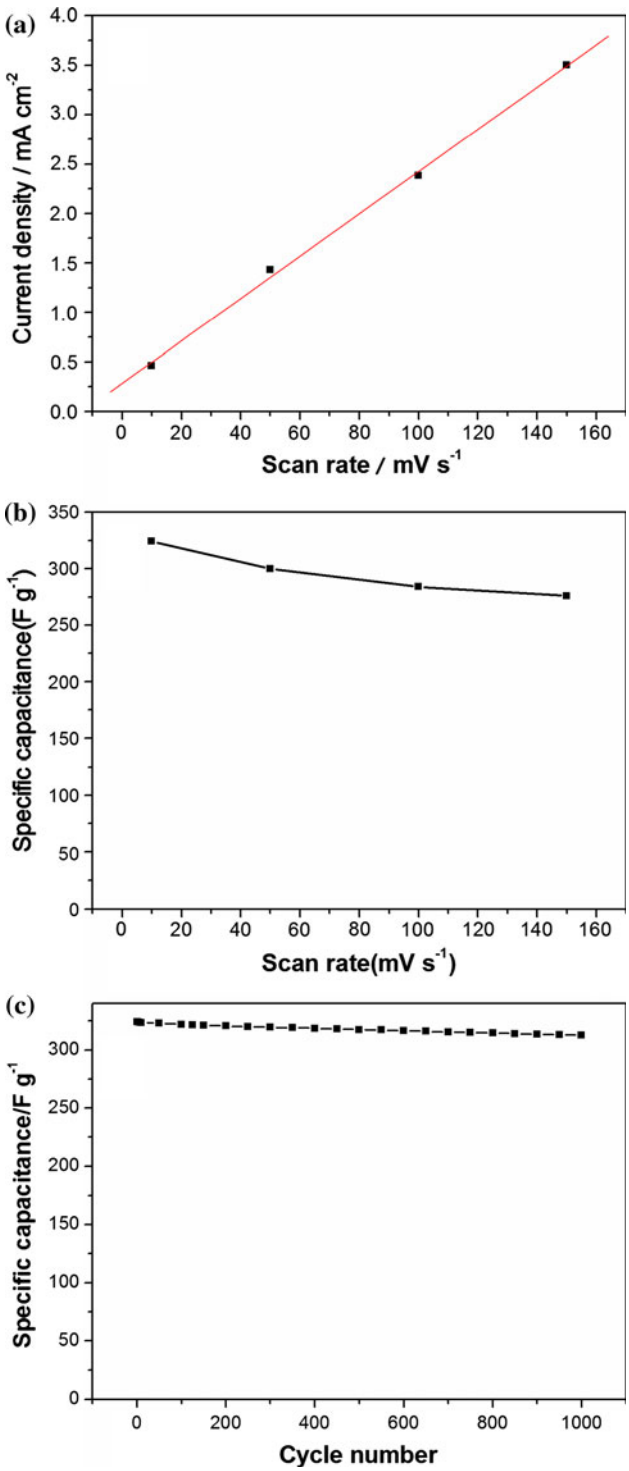

Fig. 4 **a** The dependence of the CV current density of the MnO_2/graphene composite electrode obtained at 0.5 V from the anodic branch upon CV scan rate. **b** Dependence of the specific capacitance of the MnO_2/graphene composite electrode upon CV scan rate. **c** Long-term cycle stability of the MnO_2/graphene composite electrode in 1 M Na_2SO_4 aqueous solutions at a scan rate of 10 mV s^{-1}

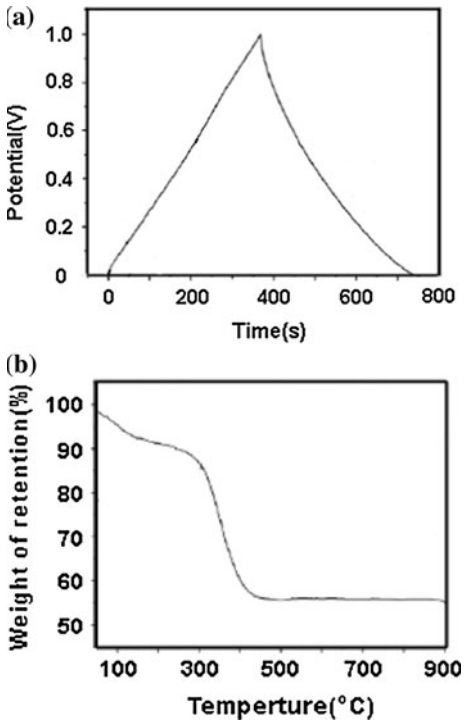

Fig. 5 **a** charge–discharge curves of MnO_2/graphene electrode at a constant current density of 1 A g^{-1}. **b** TGA curve of the MnO_2/graphene composite

capacitance of 276 F g^{-1} is obtained even at a high scan rate of 150 mV s^{-1}. Only a 15% decrease of the specific capacitance is observed from 10 to 150 mV s^{-1}. This decrease is much less than the value reported in the literature [23].

To further investigate the capacitive behavior of MnO_2/graphene electrode, galvanostatic charge/discharge measurements were performed at a constant current density of 1 A g^{-1}, within the potential range of 0–1 V. As seen from Fig. 5a, each charge–discharge curve exhibits almost linear line, indicating typical behavior of supercapacitors. The C_s is calculated according to $C_s = I \times \Delta t/(\Delta V \times m)$ from the discharge curves, where I is the constant discharge current, Δt is the discharge time, and ΔV is the potential drop during discharge. The average specific capacitances are calculated to be 325 F g^{-1} for current densities of 1 A g^{-1}, the values is consistent with the order indicated by the CVs. To clarify the contributions of MnO_2 nanoparticles and graphene nanosheets to the overall supercapacitance, we performed a thermal gravimetric analysis (TGA) on MnO_2/graphene composite (Fig. 5b). It has been determined that the composite contain 52 % MnO_2 nanoparticles. Therefore, the supercapacitance contribution of MnO_2 nanoparticles in composites can be evaluated to be 623 F g^{-1}. These results indicate that the MnO_2/graphene electrode has excellent power characteristics and is a very promising material for supercapacitor. Such a high specific capacitance indicates that MnO_2/graphene structures may be more favorable for the electron transfer reaction of electroactive compounds and MnO_2 has very high dispersibility.

The long-term cycle stability of the MnO_2/graphene composite electrode was also examined by CV at a scan rate of 10 mV s^{-1} for 1,000 cycles in 1 M Na_2SO_4 aqueous solution and the corresponding result is shown in Fig. 4c. There is only a 3.2% decrease of the specific capacitance after 1,000 cycles, which indicates that the MnO_2/graphene composite electrode has excellent long-term cycle stability.

Conclusions

MnO_2/graphene composite has been synthesized via polymer-assisted chemical reduction method. The as-prepared composite exhibited an outstanding electrochemical property as supercapacitor electrode, because of the electrochemical activities of embedded MnO_2 nanoparticles functional groups attached to graphene nanosheets, and activated graphene open network with increased specific surface area and enlarged interlayer space. These MnO_2 particles were $\sim$15 nm in size, densely distributed on graphene nanosheets, and played a crucial role in enhancing the electrochemical performance. A high specific capacitance of 324 F g^{-1} has been achieved for MnO_2/graphene composite, which is almost doubled over that of pure graphene nanosheets. In addition, the MnO_2/graphene composite electrode has excellent long-term cycle stability (only 3.2% decrease of the specific capacitance is observed after 1,000 CV cycles). Based on low cost, environmental friendly nature and excellent capacitive properties, the MnO_2/graphene composite is a promising electrode material for supercapacitors.

Acknowledgements The financial support for this work provided by the National Natural Science Foundation of China (21004009) and the Research Program of Jiangxi Province Department of Education (GJJ10093) is gratefully acknowledged.

References

1. Lee BJ, Sivakkumar SR, Ko JM, Kim JH, Jo SM, Kim DY (2007) J Power Sources 168:546
2. Hu CC, Chang KH, Wang CC (2007) Electrochim Acta 52:4411
3. Yang GW, Xu CL, Li HL (2008) Chem Comm 48:6537
4. Geim AK, Novoselov KS (2007) Nat Mater 6:183
5. Becerril HA, Mao J, Liu ZF, Stoltenberg RM, Bao Z, Chen YS (2008) ACS Nano 2:463
6. Stankovich S, Dikin DA, Piner RD, Kohlhaas KA, Kleinhammes A, Jia Y, Wu Y, Nguyen ST, Ruoff RS (2007) Carbon 45:1558
7. Yan J, Wei T, Fan ZJ, Qian WZ, Zhang ML, Shen XD, Wei F (2010) J Power Sources 195:3041
8. Wang HL, Hao QL, Yang XJ, Lu LD, Wang X (2009) Electro Comm 11:1158

9. Paek S, Yoo E, Honma I (2009) Nano Lett 9:72
10. Li F, Song J, Yang H, Gan S, Zhang Q, Han D, Ivaska A, Niu L (2009) Nanotechnology 20:455602
11. Zhang YP, Li HB, Pan LK, Lu T, Sun Z (2009) J Electroanal Chem 634:68
12. Hu CC, Tsou TW (2002) Electro Comm 4:105
13. Toupin M, Brousse T, Belanger D (2002) Chem Mater 14:3946
14. Reddy RN, Reddy RG (2003) J Power Source 124:330
15. Chen S, Zhu JW, Wu XD, Han QF, Wang X (2010) ACS Nano 4:2822
16. Kovtyukhova NI, Ollivier PJ, Martin BR, Mallouk TE, Chizhik SA, Buzaneva EV, Gorchinskiy AD (1999) Chem Mater 11:771
17. Stoller MD, Park S, Zhu Y, An J, Ruoff RS (2008) Nano Lett 8:3498
18. Ramanathan T, Abdala AA, Stankovich S, Dikin DA, Herrera-Alonso M, Piner RD, Adamson DH, Schniepp HC, Chen X, Ruoff RS, Nguyen ST, Aksay IA, Prud'Homme RK, Brinson LC (2008) Nat Nanotechnol 3:327
19. Schniepp HC, Li JL, McAllister MJ, Sai H, Herrera-Alonso M, Adamson DH, Prudhomme RK, Car R, Saville DA, Aksay IA (2006) J Phys Chem B 110:8535
20. Cheng JH, Shao G, Yu HJ, Xu JJ (2010) J Alloys Compd 505: 163
21. Gong KP, Yu P, Su L, Xiong SX, Mao LQ (2007) J Phys Chem C 111:1882
22. Liu XM, Zhang YH, Zhang XG, Fu SY (2004) Electrochim Acta 49:3137
23. Chang JK, Tsai WT (2003) J Electrochem Soc 150:A1333